

# Hydrodynamic non-linear response of interacting integrable systems

Michele Fava<sup>a,1</sup>, Sounak Biswas<sup>a</sup>, Sarang Gopalakrishnan<sup>b</sup>, Romain Vasseur<sup>c</sup>, and S. A. Parameswaran<sup>a</sup>

<sup>a</sup>Rudolf Peierls Centre for Theoretical Physics, Clarendon Laboratory, Oxford OX1 3PU, UK; <sup>b</sup>Department of Physics, The Pennsylvania State University, University Park, PA 16802, USA; <sup>c</sup>Department of Physics, University of Massachusetts, Amherst, MA 01003, USA

This manuscript was compiled on August 8, 2021

**We develop a formalism for computing the non-linear response of interacting integrable systems. Our results are asymptotically exact in the hydrodynamic limit where perturbing fields vary sufficiently slowly in space and time. We show that spatially resolved nonlinear response distinguishes interacting integrable systems from noninteracting ones, exemplifying this for the Lieb-Liniger gas. We give a prescription for computing finite-temperature Drude weights of arbitrary order, which is in excellent agreement with numerical evaluation of the third-order response of the XXZ spin chain. We identify intrinsically nonperturbative regimes of the nonlinear response of integrable systems.**

Non-linear response | Integrable systems | Generalized Hydrodynamics

Most conventional experimental probes of many-body systems, from spectroscopy to transport, operate in the linear-response regime. Linear-response coefficients such as the a.c. conductivity and dynamical susceptibility have a natural theoretical interpretation in terms of the fluctuation-dissipation theorem (1): the response to an external probe captures the intrinsic fluctuations of the system's degrees of freedom. Despite its many successes, linear response has its limitations as a probe of correlated quantum matter. For example, many different mechanisms — of varying levels of interest — give rise to incoherent spectral continua, and cannot be differentiated on the basis of linear-response data. Likewise, quantities like the conductivity probe some specific combination of the density and lifetimes of excitations; thus, e.g., the finite-frequency conductivity is qualitatively the same for a metal and an insulator. Recently, various experimental probes of *nonlinear* response have been developed to circumvent these difficulties, ranging from quench experiments in ultracold atomic gases (2) to pump-probe spectroscopy (3) and multidimensional coherent spectroscopy (4–22) in condensed-matter settings. While the first of these methods is apt for probing far-from-equilibrium dynamics and the second radically reconstructs the state of the system, the third is milder, and probes higher-order and multiple-time correlations of the equilibrium system. Such nonlinear probes are able to distinguish phases that have similar linear-response signatures: e.g., they can distinguish between excitation broadening due to disorder and that from decay (12). Despite a flurry of recent work (13–25), the theoretical toolbox for addressing nonlinear response in generic interacting quantum many-body systems is primitive, with few exact results beyond free theories and those that reduce to ensembles of two-level systems. (Notable exceptions are Refs. (26–28) which compute specific time-ordered  $n$ -point correlation functions in integrable systems with the goal of characterizing ballistic transport.)

Here, we develop and apply an asymptotically exact framework for computing the nonlinear response of interacting in-

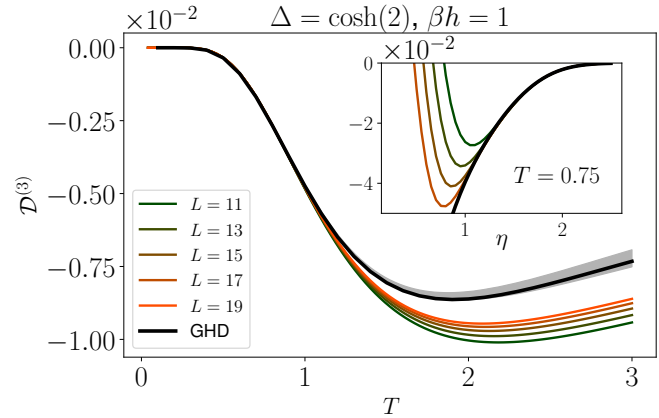


**Fig. 1.** Third-order spin Drude weight  $\mathcal{D}^{(3)}$  in the easy-axis regime of the XXZ spin chain with  $\beta h = 1$ . Main figure: Comparison between GHD and ED results for fixed  $\Delta$ . The lower (upper) boundaries of the shaded region correspond to extrapolations of finite-size ED results with a degree 1 (degree 2) polynomial in  $1/L$ . Inset:  $\mathcal{D}^{(3)}$  as a function of  $\eta = \cosh^{-1} \Delta$ .

tegrable systems, i.e. those solvable by the thermodynamic Bethe ansatz (TBA) (29). This framework is based on viewing integrability through the lens of generalized hydrodynamics (GHD) (30–32) (see also (33, 34) for a precursor of this approach, and e.g. (35–57) for recent developments); our results are exact at the hydrodynamic Euler scale, i.e. for perturba-

## Significance Statement

Studying the response of a system to external fields yields information on its macroscopic order as well as its microscopic properties. While working to linear order in field strength often suffices to describe experiments, recent advances allow measurements to probe beyond the linear regime. Understanding nonlinear response functions could significantly advance the characterization of exotic phases of matter, but little is known theoretically about their properties in interacting many-body systems. We introduce a framework for computing non-linear responses in a class of exactly solvable one-dimensional quantum systems. We show that non-linear response exhibits clear signatures of interaction effects, in contrast to linear response in similar settings.

M.F. S.B., S.G., R.V., and S.A.P. designed research; M.F. S.B., S.G., R.V., and S.A.P. performed research; M.F. S.B., S.G., R.V., and S.A.P. analyzed data; and M.F. S.B., S.G., R.V., and S.A.P. wrote the paper.

The authors declare no conflict of interest

<sup>1</sup>To whom correspondence should be addressed. E-mail: michele.fava@physics.ox.ac.uk

tions that vary slowly in space and time. [The response to sharply localized potentials could contain oscillations in space and time that the GHD approach automatically averages out and hence cannot properly capture.] We remark that with these caveats GHD, and thus our method, is believed to be exact at any finite temperature and it can be applied to the computation of correlation functions of the density of any conserved charge in any integrable system.

In the present work, we show that the nonlinear response of integrable systems contains information that is absent from (or subleading in) linear response: while the spectral functions of free and interacting integrable systems are qualitatively similar (with only subtle differences in the broadening around their ballistic light-cones (45, 46)), we find that spatially resolved nonlinear response reveals clear, qualitative distinctions between interacting and noninteracting integrable systems (as well as between chaotic and integrable systems). We discuss the prospects for measuring these features in experiments on interacting many-particle systems using nonlinear spectroscopic probes.

We also consider the generation of persistent currents after the application of an electric field, which is one of the hallmarks of integrability. At linear order in the field, the current is encoded in the linear Drude weight (36, 58). This can be readily generalized beyond the linear order, by defining higher-order Drude weights  $\mathcal{D}^{(n)}$  (59, 60). We show that our formalism yields a compact recursive formula for  $\mathcal{D}^{(n)}$  at finite temperatures. We demonstrate the validity of our hydrodynamic approach by comparing its results with those of exact diagonalization studies of integrable spin chains; we find excellent agreement (Fig. 1). We conclude by discussing the special case of the isotropic Heisenberg chain, which is known to host anomalous superdiffusive transport (61–67) characterized by propagation that is slower than ballistic motion but faster than diffusion. We show that the emergence of superdiffusion is accompanied by a breakdown of perturbation theory in the external field and hence an inherently non-perturbative nonlinear response.

## Setup

We consider general one-dimensional systems whose dynamics are governed by some integrable Hamiltonian  $H_0$ . The dynamics under  $H_0$  are treated within Euler-scale GHD (32): we partition the system into hydrodynamic cells each of mesoscopic size and linked to some spacetime point  $(x, t)$ , and assume that each cell is always instantaneously in some local generalized Gibbs ensemble (GGE) (68, 69), characterized by the vector of occupation factors of available quasiparticle states,  $\mathbf{n}(x, t) = \{n_\theta(x, t)\}$ ; the “rapidity”  $\theta$  is a convenient way of parameterizing the momentum. (We present results for systems with a single quasiparticle species but the generalization to multiple species is immediate.) The density of quasiparticles of species  $\theta$  can be expressed in terms of  $\mathbf{n}$  as  $\rho_\theta \equiv \rho_\theta^t n_\theta$ , where  $\rho_\theta^t$  is the available density of states for quasiparticles with those quantum numbers. (Note that, in an interacting system,  $\rho_\theta^t$  is itself a nontrivial function of the local GGE.) Because of integrability,  $\rho_\theta$  is separately conserved for each  $\theta$ ; moreover,  $n_\theta$  obeys a quasilinear advection equation,

$$\partial_t n_\theta + v_\theta^{\text{eff}}[\mathbf{n}] \partial_x n_\theta = 0, \quad [1]$$

where  $v_\theta^{\text{eff}}$  is an effective group velocity. In non-interacting systems, the effective velocity  $v^{\text{eff}}$  of a quasiparticle is just its group velocity. In an interacting integrable system, however, collisions are associated with a time delay in the quasiparticle trajectory, and thus renormalize the effective quasiparticle velocity.  $v^{\text{eff}}$  is therefore a nonlinear functional of  $\mathbf{n}$ .

$H_0$  has an infinite set of conserved charges,  $[H_0, \hat{Q}^j] = 0$ , whose expectation values in a GGE state are given by  $\langle \hat{Q}^j \rangle = \int dx \langle \hat{q}_j \rangle = \int dx d\theta q_\theta^j \rho_\theta$ , where  $q_\theta^j$  is the contribution to the  $j^{\text{th}}$  charge density from quasiparticle  $\theta$ . The corresponding current density is  $j_j = \int d\theta \rho_\theta q_\theta^j v_\theta^{\text{eff}}$ . GHD is highly nonlinear, even at the Euler scale, since the properties of each quasiparticle are strongly renormalized by its interactions with all the others; however, this nonlinearity can be addressed using TBA techniques.

We now discuss how external forces can be incorporated into GHD (35, 44). For concreteness we specialize to the case where the coupling is to a global  $U(1)$  charge  $\hat{q} = \hat{q}_0$ , which remains conserved even in the presence of inhomogeneous fields. Thus, the perturbed Hamiltonian is  $H(t) = \hat{H}_0 + \int dx V(x, t) \hat{q}_0(x)$ . Assuming  $V$  varies slowly in space and time, the Euler-scale time evolution of the system is described by (35, 43, 44, 47–50)

$$\partial_t n_\theta + v_\theta^{\text{eff}} \partial_x n_\theta + E a_\theta^{\text{eff}} \partial_\theta n_\theta = 0, \quad [2]$$

where  $a_\theta^{\text{eff}}[\mathbf{n}]$  is the effective acceleration of the quasiparticles, and the sole dependence on the potential is via the electric field  $E(x, t) \equiv -\partial_x V(x, t)$ . As is the case for  $v^{\text{eff}}$ ,  $a^{\text{eff}}$  is also renormalized by scattering processes and is hence a nonlinear functional of  $\mathbf{n}$ .

Finally, we note that Eq. (2) is strictly valid only at the Euler scale, i.e., for response at asymptotically large  $x$  and  $t$ , but with a fixed ratio  $x/t$ . Euler-scale response is a hallmark of integrable dynamics: chaotic systems without Galilean invariance have exponentially suppressed response at the Euler scale, since densities spread diffusively rather than ballistically. Interacting integrable systems also have diffusive corrections to ballistic quasiparticle spreading (45, 46, 70), but these corrections are also suppressed at the Euler scale.

## Nonlinear-response

Response is concerned with computing the value of some local observable  $\hat{O}$ —taken here to be a charge density  $\hat{q}_j$  or current density  $\hat{j}_j$ —following the application of electric fields  $E(x, t)$ . Since Eq. (2) is asymptotically exact at the Euler scale to all orders in  $V_j$ , it is sufficient to work perturbatively in  $V_j$  to compute the response (we comment on exceptions below). Formally, the connected order- $N$  response is

$$\chi_O^{(N)}(\{x_n, t_n\}) = \prod_{n=0}^{N-1} \frac{\delta}{\delta E(x_n, t_n)} \langle \hat{O}(x_N, t_N) \rangle \Bigg|_{E \rightarrow 0} \quad [3]$$

with  $t_0 < t_1 < \dots < t_N$ . The expectation value is taken with respect to the nonuniform state at time  $t_N$  generated by perturbing the initial uniform GGE state with external fields at times  $t_1, \dots, t_{N-1}$ . Our strategy is to express the expectation value in Eq. (3) in terms of quasiparticle occupations, perform all the functional derivatives, and then set  $E = 0$ , yielding an expression that we evaluate in the uniform GGE.

An expectation value  $\langle O(x, t) \rangle$  is a nonlinear functional of the local state  $\mathbf{n}(x, t)$ . It can be affected by perturbations at

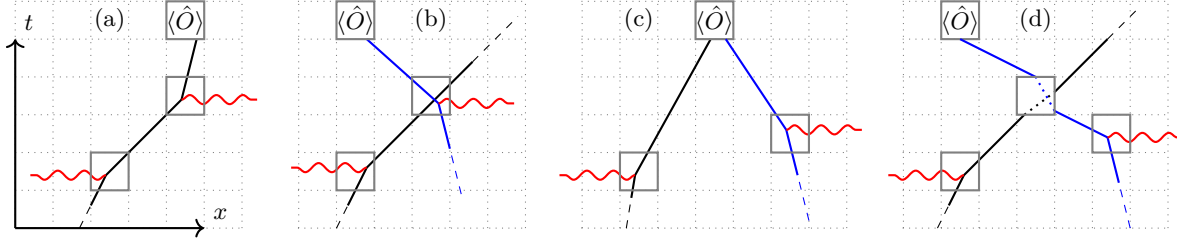


**Fig. 2.** Four distinct physical processes contributing to the second-order response  $\chi^{(2)}$ . (a) A thermal quasiparticle (QP; black line) is accelerated twice by the electric field (red wavy line), and modifies the expectation value  $\langle \hat{O} \rangle$  in the final space-time cell. (b) First a thermal QP is accelerated; a second thermal QP (blue line) is later accelerated when the first is in its space-time cell, thus modifying the effective acceleration perceived by the second; both QPs proceed ballistically and the second modifies  $\langle \hat{O} \rangle$ . (c) Two thermal QPs are independently accelerated by two pulses of the electric field; after travelling to the same space-time cell, and together they modify  $\langle \hat{O} \rangle$ . (d) As in (c), two thermal QPs are independently accelerated but one scatters off the other before influencing  $\langle \hat{O} \rangle$ . Only (a) is relevant to free systems but all four processes contribute in interacting integrable systems.

157 other spacetime points only through the advection of those  
 158 perturbations to  $(x, t)$ , which is captured by the propagator  
 159  $D_{\theta\theta'}(z, z') = \frac{\delta n_{\theta}(z)}{\delta n_{\theta'}(z')}$ , where we have defined  $z \equiv (x, t)$ . One  
 160 can express this dependence in the following compact form,  
 161 suggestive of a chain rule (71):

$$162 \quad \frac{\delta \langle \hat{O}(z_1) \rangle}{\delta E(z_0)} = \int d\theta d\alpha \frac{\delta \langle \hat{O}(z_1) \rangle}{\delta n_{\alpha}(z_1)} \frac{\delta n_{\alpha}(z_1)}{\delta n_{\theta}(z_0)} \frac{\delta n_{\theta}(z_0)}{\delta E(z_0)}, \quad [4]$$

163 Eq. (4) simply says that expectation values at spacetime point  
 164  $z_0$  depend on fields at  $z_1 \neq z_0$  purely via the process by which  
 165 the fields perturb the quasiparticle distribution at  $z_0$  and this  
 166 perturbation is advected over to  $z_1$ .

167 We are interested in generalizing Eq. (4) to the case of  
 168 higher-order functional derivatives. To organize these more  
 169 complicated expressions we have developed a diagrammatic  
 170 framework (72), which relies on the observation that any  
 171 functional derivative can be composed of the following types  
 172 of elementary object. First, there are propagators, defined  
 173 above, connecting perturbations at different spacetime points;  
 174 in a uniform GGE, the propagators take the simple form  
 175  $D_{\theta\theta'}(x_0, t_0; x_1, t_1) = \delta_{\theta\theta'} \delta[(x_0 - x_1) - v_{\theta}^{\text{eff}}(t_0 - t_1)]$  (73).  
 176 Second, there are functional derivatives of observables at a  
 177 point with respect to the quasiparticle distribution at the same  
 178 point, which can be evaluated using TBA techniques (32). We  
 179 call these “measurement vertices.” Third, there are derivatives  
 180 of the quasiparticle distribution at a spacetime point with  
 181 respect to fields at the same point. To find these we invert  
 182 Eq. (2) using Green’s function techniques, and thereby find  
 183  $\frac{\delta n_{\theta}(z)}{\delta E(z)} = -a_{\theta}^{\text{eff}}[\mathbf{n}] \partial_{\theta} n_{\theta}$  (72). We term these objects “field ver-  
 184 tices.” These three types of objects appear in Eq. (4). Finally,  
 185 response functions at order  $N > 1$  will also involve expressions  
 186 of the form  $\Gamma^{(p)} = \frac{\delta^p n_{\theta}(z_0)}{\delta n_{\theta_1}(z_1) \dots \delta n_{\theta_p}(z_p)}$ . These capture the modi-  
 187 fication of the spacetime propagator by scattering events, and  
 188 can be computed by repeatedly differentiating Eq. (1) with  
 189 respect to  $n$ , which yields a recursive formula, that allows us  
 190 to express  $\Gamma^{(p)}$  in terms of  $\partial_x \Gamma^{(1)}$  and functional derivatives of  
 191 the  $v^{\text{eff}}[\mathbf{n}]$  with respect to quasiparticle occupations (72). We  
 192 refer to these objects as “scattering vertices.” All other types  
 193 of object can be expressed in terms of these: e.g., functional  
 194 derivatives of the form  $\frac{\delta^k \langle \hat{O} \rangle}{\delta n_{\theta_1}(z_1) \dots \delta n_{\theta_k}(z_k)}$ , can be rewritten in  
 195 terms of measurement or scattering vertices and propagators,  
 196 which advect all occupation factors to the point where the  
 197 functional derivative is taken. We may verify that for  $N = 1$   
 198 this procedure yields the standard expressions for linear re-

sponse. Higher-order response functions can then be computed  
 199 recursively from Eq. (3). 200

201 Although the formal expressions rapidly become unwieldy  
 202 with increasing  $N$ , they have a transparent physical interpre-  
 203 tation, as we now exemplify for  $N = 2$ . The external field  
 204 can affect the system via two distinct physical processes, each  
 205 corresponding to a distinct field vertex (represented by a box  
 206 with a wavy line in Fig. 2): it can accelerate a thermal quasi-  
 207 particle from rest within a spacetime cell (the first field vertex  
 208 in Fig. 2a), or else accelerate a quasiparticle previously acted  
 209 upon by the field at an earlier time (the second field vertex  
 210 in Fig. 2a). In a non-interacting integrable system different  
 211 quasiparticles are independent of each other, thus all con-  
 212 nected nonlinear response functions result solely when a single  
 213 quasiparticle is repeatedly accelerated by the field, and then  
 214 measured, as in Fig. 2a. However, in interacting integrable  
 215 systems, quasiparticles influence each other via scattering  
 216 processes. Consequently, the ability of the field to excite a  
 217 quasiparticle in a given spacetime cell  $z$  is also sensitive to the  
 218 presence of quasiparticles excited by the field in all spacetime  
 219 cells in the past light-cone of  $z$  under the advective dynamics  
 220 of GHD, leading to additional connected contributions (as in  
 221 Fig. 2b). Quasiparticles excited by the field acting at distinct  
 222 spacetime cells can also propagate to a single cell where they  
 223 jointly modify the measured observable (Fig. 2c). Interactions  
 224 thus lead to an infinite hierarchy of field and measurement  
 225 vertices, that are sensitive to the presence of an increasing  
 226 number of previously-excited quasiparticles in the spacetime  
 227 cells where quasiparticles are accelerated or measured. Finally,  
 228 the nonlinear response also receives contributions from scatter-  
 229 ing vertices, again of arbitrary order, due to the phase shift  
 230 experienced by the measured quasiparticle as it propagates be-  
 231 tween the acceleration and measurement cells in the presence  
 232 of other excited quasiparticles in the system (Fig. 2d). The  
 233  $N^{\text{th}}$  order response in an interacting integrable system involves  
 234  $N$  field vertices and a single measurement vertex, linked by  
 235 advection propagators  $D_{\theta\theta'}(z, z')$  and scattering vertices, and  
 236 can be organized using spacetime diagrams (72). Crucially, at  
 237 fixed  $N$ , only vertices below some finite order can contribute:  
 238 for instance Fig. 2 contains all processes contributing to  $\chi^{(2)}$ . 239

240 We caution the reader that in Fig. 2 the effects of fields and  
 241 collisions are exaggerated for clarity. In fact, the trajectory  
 242 shift due to scattering processes as in Fig. 2d is infinitesimal,  
 243 and similarly a perturbing external field only imparts an in-  
 244 finitesimal acceleration to each quasiparticle. Thus there are  
 kinematic restrictions on allowed processes that the figure does

not capture. For instance, the process in Fig. 2a is possible only if the three points — the two where the field act and the one at which the measurement occurs — lie on the same ray  $x = x_0 + v\lambda t$  for some initial position  $x_0$  and some rapidity  $\lambda$ . This aspect will be crucial to our discussion in the next section.

## Measuring Interactions in the Lieb-Liniger Gas

As an example of this approach, we apply it to the Lieb-Liniger model of 1D bosons with contact interactions,

$$\hat{H}_0 = \frac{1}{2} \sum_j \hat{p}_j^2 + c \sum_{i \neq j} \delta(\hat{x}_i - \hat{x}_j), \quad [5]$$

where  $\hat{x}_j$  and  $\hat{p}_j$  are the position and momentum of particle  $j$ . The bare group velocity  $v$  of a particle is equal to its momentum  $p$ . The effective velocity  $v^{\text{eff}}$  can be obtained from  $v$  as the solution to an integral equation, whose explicit form is provided in the Methods section. An additional fact, peculiar to the Lieb-Liniger gas, is that the effective acceleration  $a^{\text{eff}}$  is not renormalized by interactions; with our choice of conventions,  $a^{\text{eff}} = 1$ . For  $c \rightarrow 0$ ,  $\hat{H}_0$  is a free Bose gas, while for  $c \rightarrow \infty$  it can be described as a theory of free fermions. This can be recognized, for example, by studying  $v^{\text{eff}}$ , which in both limits tends to the bare group velocity  $v$ . Consequently linear response in these two limits approximates that of free bosons or fermions respectively, with only quantitative corrections from interactions. This hinders a precise measurement of  $c$  based only on linear response. We now demonstrate that a spatially-resolved measurement of  $\chi^{(2)}$  —or higher-order responses— carries direct information about the interactions. For concreteness, we consider a specific charge response of the form  $\tilde{\chi}^{(2)}(x, t, \tau) \equiv \chi_{\hat{q}_0}^{(2)}(0, 0; x, \tau; 0, \tau + t)$  where the first perturbation and the measurement coincide spatially, and the system is perturbed at an intermediate time at position  $x$ . In the free boson or free fermion limits, we know from the discussion in the previous section that the only process contributing to  $\chi^{(2)}$  is one where a single quasiparticle is repeatedly accelerated by the subsequent field applications (Fig. 2a). Furthermore, as previously noted, this process can take place only if all the points in which the perturbation is applied and the measurement point lie on the same ray. Thus, in the two non-interacting limits  $\tilde{\chi}^{(2)}(x, t, \tau)$  will vanish everywhere except at  $x = 0$ . Conversely, if  $c = O(1)$ , quasiparticles are strongly interacting, and each influences the dynamics of the others. For example, processes such as those in Fig. 2d will be non-zero since  $v^{\text{eff}}$  of a quasiparticle with momentum  $p$  will depend on all the quasiparticles in the same region. (72) We thus expect that  $\chi^{(2)}$  is generically finite and non-zero for arbitrary perturbation and measurement points.

To summarize: if we focus on the region away from  $x = 0$ , i.e. chosen to exclude the case where all points lie along the same ray, we expect  $\tilde{\chi}^{(2)}(x, t, \tau)$  to be directly sensitive to the interactions, and hence generically will have a nonzero value away from the free limits  $c \rightarrow 0$  or  $c \rightarrow \infty$ . An immediate corollary is that in these limits,  $\tilde{\chi}^{(2)}(x \neq 0, t, \tau)$  should respectively vanish as  $O(c)$  or  $O(1/c)$ . This should be contrasted with linear response measurements where  $\chi^{(2)} = O(1)$  in all these cases and the effect of interactions is to determine sub-leading corrections.

Indeed, this response is readily computed using the above formalism (as detailed in the Methods section and (72)); Fig. 3

shows the results for various interaction strengths, at fixed temperature  $T$  and boson density  $\bar{n}$ . As  $c$  decreases we see that the signal moves closer to  $x = 0$ . This is because for  $c \rightarrow 0$  the system is proximate to a Bose-Einstein condensate at  $c = 0$  and  $T = 0$  (see e.g. Refs. (74, 75)), and hence only slow, low momentum quasiparticle states are occupied. [See the Methods for another effect contributing to the signal moving near  $x = 0$ .] Furthermore, note that the signal starts to decrease either for  $c \lesssim 10^{-2}$  or  $c \gtrsim 1$ , as expected. [Recovering free boson response as  $c \rightarrow 0$  requires studying very low  $c$ ; as  $c$  decreases, the density of states initially increases due to the incipient Bose condensation, enhancing interaction effects.] These observations are not restricted to the protocol analyzed above: any protocol which separates the same-ray ‘free’ contribution from the regular part of the response would yield similar results. Thus, nonlinear correlators provide a more direct window into the interacting Lieb-Liniger gas than linear response.

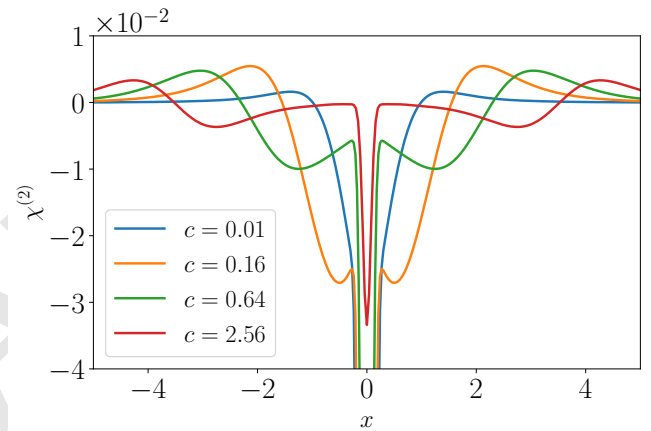


**Fig. 3.**  $\chi^{(2)}(0, 0; x, \tau; 0, \tau + t)$  in the Lieb-Liniger model for various interaction strengths  $c$ . We take  $T = 2$ ,  $\bar{n} = 1$ ,  $\tau = t = 1$  and regularize the  $\delta$ -function GHG propagator as a Gaussian of width  $\eta = 0.1$ . In a noninteracting system, the only response would come from the resolution-limited spike at  $x_1 = 0$ ; everything else is a signature of interactions.

In passing, note that spatially-resolved measurements of multi-point nonlinear response would also give a powerful diagnostic for ballistic transport, and hence integrability. As we remarked above, the existence of nontrivial Euler-scale response—absent strict Galilean invariance—is a hallmark of integrable dynamics, and suffices to diagnose integrability. Even in Galilean-invariant chaotic fluids with a few conserved currents, quasiparticles propagate sub-ballistically, so one expects an Euler-scale multi-point correlator like that shown in Fig. 3 to be strongly suppressed relative to the integrable case.

## Higher-order Drude weights

So far, we have focused on spatially-resolved response. While this can be measured in cold-atom experiments, most solid-state spectroscopic techniques only access spatially integrated quantities. At the Euler scale, the most natural integrated quantity is the generation of a persistent current in response to a uniform electric field. This follows from the fact that the current operator in an integrable system generically has some part that is strictly conserved under time evolution, so the current generated in response to an electric field will

not decay over time. For example, specializing to first-order response,  $\int dx \chi_{j_0}^{(1)}(0, 0; x, t)$  will tend to a constant as  $t \rightarrow \infty$ ; this limiting value is called the Drude weight (76, 77). Alternatively, in frequency space, the conductivity goes as  $\sigma(\omega) = \pi \mathcal{D} \delta(\omega) + \dots$ . Drude weights extend to nonlinear response: a field  $E$  applied to the system for a finite time  $\Delta t$  drives a persistent current  $j_0(\varphi)$ , where  $\varphi \equiv E \Delta t$  is the vector potential variation due to the field. By expanding  $j_0(\varphi)$  as a series in its argument and taking derivatives, we may define a sequence of nonlinear Drude weights (59, 60) (which can be defined similarly for any other operator).

Our diagrammatic approach can straightforwardly be used to compute  $N^{\text{th}}$  order Drude weights  $\mathcal{D}^{(N)}$ , by integrating the  $N^{\text{th}}$  order response over the positions of the field insertions. As shown in the SM (72), this yields the recursive formula

$$\mathcal{D}_{\hat{O}}^{(N)} = - \int d\theta_N a^{\text{eff}} \partial_{\theta_N} n \frac{\delta}{\delta n_{\theta_N}} \mathcal{D}_{\hat{O}}^{(N-1)}, \quad [6]$$

with  $\mathcal{D}^{(0)} = \langle \hat{O} \rangle$ . This recursive formula allows to obtain a closed-form expression for non-linear Drude weight of arbitrary order only using TBA technology, with explicit expressions up to third order given in the SM (72).

While Eq. (6) rapidly becomes complex with increasing  $N$ , a simple limit emerges for the first term of a high-temperature expansion: since each factor of  $\partial_{\theta} n$  is proportional to  $T^{-1}$ , the leading contribution to  $\mathcal{D}_{\hat{O}}^{(N)}$  is always obtained by acting with  $\frac{\delta}{\delta n_{\theta_N}}$  on the factor  $\partial_{\theta_{N-1}} n_{\theta_{N-1}}$  in  $\mathcal{D}_{\hat{O}}^{(N-1)}$ . Integrating by parts, we find that as  $T \rightarrow \infty$ ,

$$\mathcal{D}_{\hat{O}}^{(N)} = - \int d\theta \partial_{\theta} n \left[ a^{\text{eff}} \frac{\partial}{\partial \theta} \right]^{N-1} a^{\text{eff}} \frac{\delta \langle \hat{O} \rangle}{\delta n(\theta)} + O(T^{-2}). \quad [7]$$

We benchmark this GHD result against numerical simulations of a paradigmatic integrable model, the XXZ spin chain, and focus on spin current response. Since spatial inversion symmetry forces spatially-averaged current response functions to vanish for any even  $N$ , we focus on  $\mathcal{D}^{(3)}$ . We work in the easy-axis limit, and exploit the generalized Kohn formula (59, 60) combined with exact diagonalization (ED) on small systems. (Unfortunately, state-of-the-art matrix product operator techniques for linear Drude weights (78) do not give comparably good results for higher-order Drude weights (72).) Our results are presented in Fig. 1; despite the difficulty of extrapolating reliably to the thermodynamic limit from the small system sizes accessible to ED, we see that the GHD results are within the range of our extrapolations at high temperature, and agree extremely well at lower temperatures. We also see good agreement as we vary the easy-axis anisotropy at fixed temperature.

## Discussion

In this work we have presented a general framework for computing nonlinear response within GHD, demonstrated that it is in excellent agreement with exact numerics, and illustrated how it can directly distinguish between free and interacting integrable systems. Our results suggest a natural experimental protocol for directly measuring quasiparticle interaction effects in the Lieb-Liniger model using ultracold atomic gases. (Importantly, this approach does not require single-site imaging resolution.) Since our proposal involves *finite-time* behavior, it can be applied to realistic experimental settings where integrability is only approximate. We have focused on regimes where

the nonlinear response is perturbative, and can be expanded in powers of the field strength. In such regimes, our results for nonlinear response bear some resemblance to those for full counting statistics (26–28). The multipoint correlators that appear in that theory (with all operators evaluated at the same point in space) are a special case of those computed here.

We need not look far for integrable systems in which response is inherently *nonperturbative*. The most transparent example is the isotropic Heisenberg model, at  $h = 0$ . In linear response, this model exhibits anomalous transport in the Kardar-Parisi-Zhang universality class (61–67). We may approach this regime from nonzero  $\beta h$  by taking appropriate limits. Explicitly computing the spin current due to an impulse  $\varphi = E \Delta t$ , we find that

$$J(h, \varphi) \approx h \sum_{s=1}^{1/h} s^{-4} f(h\varphi s^3), \quad [8]$$

for some scaling function  $f$  that is approximately sinusoidal in its argument (72). The sum is over quasiparticle “strings”, which are bound states of  $s$  elementary magnons. If we now take  $\varphi \rightarrow 0$  at fixed  $h \neq 0$ , we obtain a series in powers of  $\varphi$ , where the first term is the linear Drude weight ( $\varphi \mathcal{D}^{(1)} \sim \varphi h^2 |\log h|$ ), the next nonvanishing term is  $\varphi^3 \mathcal{D}^{(3)} \sim \varphi^3 / h^2$ , and higher-order terms are even more singular in the half-filling limit. The  $\varphi \rightarrow 0$  and  $h \rightarrow 0$  limits strikingly fail to commute: if we instead take  $h \rightarrow 0$  at fixed  $\varphi$ , we find that  $J(h, \varphi) \sim h^2 \varphi |\log h \varphi|$ . In effect,  $\varphi$  can act as a *cutoff* on response: for any fixed field, sufficiently large bound states respond nonperturbatively and undergo Bloch oscillations. A proper description of such nonperturbative phenomena requires extending the present framework beyond Euler scale, e.g., by including diffusive corrections (45, 46, 70) and other sources of irreversibility (79). We leave this as an important direction for future work.

*Note added.*— As this paper was being completed we became aware of recent work (80) that computes exact non-linear Drude weights for the XXZ chain. Ref. (80) considers only  $T = 0$  and  $|\Delta| < 1$ , and hence has limited overlap with the results presented here. We have checked that our results for  $T \rightarrow 0$  agree in the relevant regime of  $\Delta$ . Since the issue of irreversibility for finite- $T$  GHD calculations is particularly challenging to address in the easy-plane regime for reasons noted in Ref. (79), we defer detailed study of this regime to future work.

## Materials and Methods

**Computation of  $\Gamma^{(2)}$ .** In this subsection, we describe how  $\Gamma^{(2)} = \frac{\delta^2 n_{\theta}(z)}{\delta n_{\theta_1}(z_1) \delta n_{\theta_2}(z_2)}$  can be expressed in terms of linear propagators  $D$  and a scattering vertex. For the most general case of  $\Gamma^{(p)}$ , we refer the reader to the SM (72).

To compute  $\Gamma^{(2)}$  we take the functional derivative of Eq. (1) w.r.t.  $n(x_0, t_0)$  and  $n(x_1, t_1)$ , and evaluate it on top of a homogeneous background, obtaining

$$\begin{aligned} & (\partial_t + v_{\theta}^{\text{eff}} \partial_x) \Gamma^{(2)} = \\ & = - \left( \int d\theta' \frac{\delta v_{\theta}^{\text{eff}}}{\delta n_{\theta'}} D_{\theta', \theta_1}(z_1, z) \partial_x D_{\theta, \theta_0}(z_0, z) + (0 \leftrightarrow 1) \right). \quad [9] \end{aligned}$$

Note that, since we have now fixed  $\mathbf{n}$  to be the uniform thermal background, we have dropped terms proportional to  $\partial_x n$ . The LHS of this equation consists of  $\Gamma^{(2)}$  acted upon by a linear partial differential operator (PDO) [since  $\mathbf{n}$  is now fixed to be the thermal background] whose Green's function is given by the propagator  $D$ . Inverting the PDO using its Green's function, we have

$$\Gamma^{(2)} = -\delta_{\theta, \theta_2} \int d^2 z_s D_{\theta}(z_s, z) \frac{\delta v_{\theta}^{\text{eff}}}{\delta n_{\theta_1}} D_{\theta_1}(z_1, z) \partial_x D_{\theta}(z_0, z) + (0 \leftrightarrow 1) \quad [10]$$

where we introduced  $D_{\theta}(z_0, z_1) = \delta(x_1 - x_0 - v_{\theta}^{\text{eff}}(t_1 - t_0))$ ,  $z_s = (x_s, t_s)$  labelling the position of the scattering process, and  $d^2 z_s = dx_s dt_s$ .

In this expression we can recognize the structure of a process like that depicted in Fig. 2d. Note that  $\frac{\delta v_{\theta}^{\text{eff}}}{\delta n_{\theta_1}}$  and hence  $\Gamma^{(2)}$  will be non-zero only if the model is interacting; in a free theory  $v^{\text{eff}}$  reduces to the group velocity and will hence be independent of  $n_{\theta_1}$ .

**$\chi^{(2)}$  in the Lieb-Liniger model.** In this section we focus on the protocol described in the Section "Measuring interactions in the Lieb-Liniger gas" and the corresponding computation of  $\chi_{\hat{q}_0}^{(2)}(0, 0; x, \tau; 0, \tau + t)$ . In particular, for  $x \neq 0$ ,  $\chi^{(2)}$  is given by the sum of two contributions, represented in Fig. 2(c-d). In fact, (a) is zero whenever  $x \neq 0$ , and (b) is zero in the Lieb-Liniger model since  $a^{\text{eff}} = 1$  and does not carry any dependence on the state  $n$ .

For continuity with the previous section, we focus on contribution (d), which is given by

$$\chi_d^{(2)} = \int d\theta d\theta_1 d\theta_2 a_{\theta_1}^{\text{eff}} \partial_{\theta} n_{\theta_1} a_{\theta_2}^{\text{eff}} \partial_{\theta} n_{\theta_2} \Gamma^{(2)} \frac{\delta \langle \hat{O} \rangle}{\delta n(\theta)}, \quad [11]$$

where  $\Gamma^{(2)} = \frac{\delta n_{\theta}(0, t + \tau)}{\delta n_{\theta_1}(0, 0) \delta n_{\theta_2}(x, \tau)}$  is given in the previous section in terms of  $\frac{\delta v_{\theta}^{\text{eff}}}{\delta n_{\theta_1}}$ . In the Lieb-Liniger model the momentum corresponds to the rapidity  $k = \theta$  and the energy is given by  $e = k^2/2$  [as customary, we are choosing units in which the mass of the particles is 1]. The bare group velocity is then given by  $v_{\theta} = k = \theta$ . The effective group velocity, which is renormalized by the interactions is then given by the solution of the integral equation (32)

$$\rho_{\theta}^{\dagger} v_{\theta}^{\text{eff}} = \rho_{\theta}^{\dagger} v_{\theta} + \int d\theta' K_{\theta - \theta'} n_{\theta'} \rho_{\theta'}^{\dagger} v_{\theta'}^{\text{eff}}. \quad [12]$$

$K_{\theta - \theta'}$  is the so-called scattering kernel, which encodes the phase shifts (or equivalently time delays) of quasiparticles upon scattering. In the Lieb-Liniger model it takes the form

$$K_{\theta - \theta'} = \frac{1}{\pi} \frac{c}{(\theta - \theta')^2 + c^2}. \quad [13]$$

Before separately analysing the two limits  $c \rightarrow 0$  and  $c \rightarrow \infty$ , we report the free particle result, which holds both for free fermions or bosons, and is entirely due to diagram (a):

$$\chi_a^{(2)} = \int \frac{dp}{2\pi} \frac{\delta \langle \hat{O} \rangle}{\delta n_p} D_p(z_2, z_1) a_p \partial_p (D_p(z_1, z_0) a_p \partial_p n_p). \quad [14]$$

As previously noted, the products  $D_p(z_2, z_1) D_p(z_1, z_0)$  and  $D_p(z_2, z_1) \partial_p D_p(z_1, z_0)$  vanishes whenever all the points  $\{z_0, z_1, z_2\}$  do not lie on the same ray. Finally, we can see that the only difference between fermions and bosons is in the dependence of  $n_p$ , i.e.

$$n_p = \frac{1}{1 \pm e^{\beta(e_p - \mu)}}, \quad [15]$$

in the two cases.

For the Lieb-Liniger has, it is easiest to recover this form in the free-fermion limit  $c \rightarrow \infty$ , in which  $K_{\theta - \theta'} \rightarrow 0$ . In this case, it is then clear that  $v_p^{\text{eff}} \rightarrow v_p = p$  independently of the state  $n_{\theta}$ . As a consequence  $\frac{\delta v_{\theta}^{\text{eff}}}{\delta n_{\theta_1}} \rightarrow 0$  and  $\Gamma^{(2)}$  will vanish.

The free-boson limit  $c \rightarrow 0$  of the Lieb-Liniger gas is more subtle. The key observation is that the width of the function  $K_{\theta - \theta'}$  is

proportional to  $c$ . Combining this observation with Eq. Eq. (12) we expect that  $\frac{\delta v_{\theta}^{\text{eff}}}{\delta n_{\theta_1}}$  will be non-negligible only if  $\theta - \theta_1 \lesssim c$ . Looking at Fig. 2(d), note that the slope of the black trajectory is given by  $v^{\text{eff}}(\theta_1)$ , while the slope of the blue one is  $v^{\text{eff}}(\theta)$ . Thus, as  $c \rightarrow 0$ , for an effective scattering process to take place  $v^{\text{eff}}(\theta) - v^{\text{eff}}(\theta_1) = O(c)$ , requiring that the three points lie approximately on the same ray, i.e.  $x = O(c)$ . We can then see that ultimately this contribution will be peaked in the same region where diagram (a) is non-zero and it will be impossible to separate them. Similar considerations would also hold for diagram (c).

While the above discussion implies that  $\tilde{\chi}^{(2)}(x \neq 0, t, \tau)$  tends to zero in the  $c \rightarrow 0$  limit, as it should for a free-particle system, it is not immediately clear analytically that the signal at  $x = 0$  tends to its free boson value. This can, however, be verified numerically, by showing that the sum of diagrams (c), and (d) in Fig. 2 tends to zero as  $c \rightarrow 0$ .

**Numerical computation of the non-linear Drude weights.** In our numerical calculations we used the generalized Kohn formula (59, 60) combined with exact diagonalization. The generalized Kohn formula relates the current Drude weights to the derivatives of the energy levels when a gauge flux  $\varphi$  is threaded through a system with periodic boundary conditions. E.g. for  $\mathcal{D}_{\hat{J}_0}^{(3)}$  it gives

$$\mathcal{D}_{\hat{J}_0}^{(3)} = \frac{1}{L} \sum_n p_n \frac{d^4 \epsilon_n}{d\varphi^4} = \frac{1}{L} \sum_n p_n \frac{d^3 \langle \hat{J}_0 \rangle_n}{d\varphi^3}, \quad [16]$$

where  $L$  denotes the length of the system,  $n$  runs over the eigenstates of  $\hat{H}_0$ , each of whom has energy  $\epsilon_n$  and is occupied with probability  $p_n$ . In the second part  $\hat{J}_0$  is the total charge current  $\sum_j \hat{j}_0(j)$  and  $\langle \cdot \rangle_n$  denotes the average over the  $n$ -th eigenstate. The figures reported in the main text are obtained by summing over all symmetry sectors (momentum and magnetization).

Note that a naive implementation of this formula based on finite differences would be problematic. For small enough  $\varphi$  the numerical precision on the finite difference (which must be divided by  $\varphi^3$ ) would limit the accuracy of the results. On the other hand, at large enough  $\varphi$ , level crossings start to occur, thus compromising the results. Empirically, it seems that these two problems significantly compromise the results for all values of  $\varphi$  starting at  $L \gtrsim 15$ . There are two possible solutions to this problem. One is to use perturbation theory to express  $\frac{d^4 \epsilon_n}{d\varphi^4}$  based on matrix elements of  $\hat{H}_0$  and  $\hat{J}_0$  (see Eq. (31) of Ref. (60)). Another alternative exploits the integrability of the model in question. In fact, we could choose a large  $\varphi \simeq 10^{-2}$ , and track levels through the various crossings based on their fidelity  $\langle n(\varphi_0) | n(\varphi_1) \rangle$ . Both approaches give consistent results for the cases we considered.

Finally, we point out that this approach is heavily limited by finite-size effects, specifically at small  $|\Delta| - 1$  or medium-high temperatures, where a reliable extrapolation to the thermodynamic limit is not possible (72).

**ACKNOWLEDGMENTS.** We thank Bruno Bertini for insightful discussions. We acknowledge support from NSF Grant No. DMR-1653271 (S.G.), the European Research Council under the European Union Horizon 2020 Research and Innovation Programme via Grant Agreement No. 804213-TMCS (S.A.P., S.B.), the US Department of Energy, Office of Science, Basic Energy Sciences, under Early Career Award No. DE-SC0019168 (R.V.), and the Alfred P. Sloan Foundation through a Sloan Research Fellowship (R.V.).

1. PC Martin, *Measurements and correlation functions*. (CRC Press), (1968).
2. I Bloch, J Dalibard, W Zwerger, Many-body physics with ultracold gases. *Rev. Mod. Phys.* **80**, 885–964 (2008).
3. A Cavalleri, et al., Femtosecond structural dynamics in  $\text{VO}_2$  during an ultrafast solid-solid phase transition. *Phys. Rev. Lett.* **87**, 237401 (2001).
4. S Mukamel, *Principles of nonlinear optical spectroscopy*. (Oxford University Press on Demand) No. 6, (1999).
5. SA Lynch, et al., First observation of a THz photon echo in *35th International Conference on Infrared, Millimeter, and Terahertz Waves*. (IEEE), pp. 1–2 (2010).
6. J Lu, et al., Nonlinear two-dimensional terahertz photon echo and rotational spectroscopy in the gas phase. *Proc. Natl. Acad. Sci.* **113**, 11800–11805 (2016).

- 557 7. H Hirori, A Doi, F Blanchard, K Tanaka, Single-cycle terahertz pulses with amplitudes exceeding 1 MV/cm generated by optical rectification in LiNbO<sub>3</sub>. *Appl. Phys. Lett.* **98**, 091106 (2011).
- 558
- 559
- 560 8. W Kuehn, K Reimann, M Woerner, T Elsaesser, R Hey, Two-Dimensional Terahertz Correlation Spectra of Electronic Excitations in Semiconductor Quantum Wells. *J. Phys. Chem. B* **115**, 5448–5455 (2011).
- 561
- 562
- 563 9. P Jepsen, et al., Ultrafast carrier trapping in microcrystalline silicon observed in optical pump–terahertz probe measurements. *App. Phys. Lett.* **79**, 1291 (2001).
- 564
- 565 10. M Woerner, W Kuehn, P Bowlan, K Reimann, T Elsaesser, Ultrafast two-dimensional terahertz spectroscopy of elementary excitations in solids. *New J. Phys.* **15**, 025039 (2013).
- 566
- 567 11. J Lu, et al., Coherent Two-Dimensional Terahertz Magnetic Resonance Spectroscopy of Collective Spin Waves. *Phys. Rev. Lett.* **118**, 207204 (2017).
- 568
- 569 12. F Mahmood, D Chaudhuri, S Gopalakrishnan, R Nandkishore, NP Armitage, Observation of a marginal fermi glass. *Nat. Phys.* **17**, 627–631 (2021).
- 570
- 571 13. Y Wan, N Armitage, Resolving Continua of Fractional Excitations by Spinon Echo in THz 2D Coherent Spectroscopy. *Phys. Rev. Lett.* **122**, 257401 (2019).
- 572
- 573 14. SA Parameswaran, S Gopalakrishnan, Asymptotically exact theory for nonlinear spectroscopy of random quantum magnets. *Phys. Rev. Lett.* **125**, 237601 (2020).
- 574
- 575 15. RM Nandkishore, W Choi, YB Kim, Spectroscopic fingerprints of gapped quantum spin liquids, both conventional and fractonic. *Phys. Rev. Res.* **3**, 013254 (2021).
- 576
- 577 16. R Nandkishore, S Gopalakrishnan, Lifetimes of local excitations in disordered dipolar quantum systems. *Phys. Rev. B* **103**, 134423 (2021).
- 578
- 579 17. Y Michishita, R Peters, Correlation effect on nonlinear responses in strongly-correlated electron systems. *arXiv e-prints*, arXiv:2012.10603 (2020).
- 580
- 581 18. SM João, JMVP Lopes, Basis-independent spectral methods for non-linear optical response in arbitrary tight-binding models. *J. Physics: Condens. Matter* **32**, 125901 (2019).
- 582
- 583 19. W Choi, KH Lee, YB Kim, Theory of two-dimensional nonlinear spectroscopy for the Kitaev spin liquid. *Phys. Rev. Lett.* **124**, 117205 (2020).
- 584
- 585 20. M Kanega, TN Ikeda, M Sato, Linear and Nonlinear Optical Responses in Kitaev Spin Liquids. *arXiv e-prints*, arXiv:2101.06081 (2021).
- 586
- 587 21. T Holsten, M Krüger, A Thermodynamic Non-Linear Response Relation. *arXiv e-prints*, arXiv:2101.05019 (2021).
- 588
- 589 22. I Paul, Nonlinear terahertz electro-optical responses in metals. *arXiv e-prints*, arXiv:2101.04136 (2021).
- 590
- 591 23. I Sodemann, L Fu, Quantum nonlinear hall effect induced by berry curvature dipole in time-reversal invariant materials. *Phys. Rev. Lett.* **115**, 216806 (2015).
- 592
- 593 24. DE Parker, T Morimoto, J Orenstein, JE Moore, Diagrammatic approach to nonlinear optical response with application to weyl semimetals. *Phys. Rev. B* **99**, 045121 (2019).
- 594
- 595 25. Z Li, T Tohyama, T Itaka, H Su, H Zeng, Nonlinear optical response from quantum kinetic equation. *arXiv e-prints*, arXiv:2001.07839 (2020).
- 596
- 597 26. B Doyon, J Myers, Fluctuations in ballistic transport from euler hydrodynamics. *Annales Henri Poincaré* **21**, 255–302 (2019).
- 598
- 599 27. J Myers, MJ Bhaseen, RJ Harris, B Doyon, Transport fluctuations in integrable models out of equilibrium. *SciPost Phys.* **8**, 7 (2020).
- 600
- 601 28. G Peretto, B Doyon, Euler-scale dynamical fluctuations in non-equilibrium interacting integrable systems. *arXiv e-prints*, arXiv:2012.06496 (2020).
- 602
- 603 29. M Takahashi, *Thermodynamics of one-dimensional solvable models*. (Cambridge university press), (2005).
- 604
- 605 30. OA Castro-Alvaredo, B Doyon, T Yoshimura, Emergent hydrodynamics in integrable quantum systems out of equilibrium. *Phys. Rev. X* **6**, 041065 (2016).
- 606
- 607 31. B Bertini, M Collura, J De Nardis, M Fagotti, Transport in Out-of-Equilibrium  $XXZ$  Chains: Exact Profiles of Charges and Currents. *Phys. Rev. Lett.* **117**, 207201 (2016).
- 608
- 609 32. B Doyon, Lecture Notes On Generalised Hydrodynamics. *SciPost Phys. Lect. Notes*, 18 (2020).
- 610
- 611 33. S Sachdev, K Damle, Low Temperature Spin Diffusion in the One-Dimensional Quantum O(3) Nonlinear  $\sigma$  Model. *Phys. Rev. Lett.* **78**, 943–946 (1997).
- 612
- 613 34. K Damle, S Sachdev, Spin dynamics and transport in gapped one-dimensional Heisenberg antiferromagnets at nonzero temperatures. *Phys. Rev. B* **57**, 8307–8339 (1998).
- 614
- 615 35. B Doyon, T Yoshimura, A note on generalized hydrodynamics: inhomogeneous fields and other concepts. *SciPost Phys.* **2**, 014 (2017).
- 616
- 617 36. B Doyon, H Spohn, Drude Weight for the Lieb-Liniger Bose Gas. *SciPost Phys.* **3**, 039 (2017).
- 618
- 619 37. E Ilievski, J De Nardis, Ballistic transport in the one-dimensional hubbard model: The hydrodynamic approach. *Phys. Rev. B* **96**, 081118 (2017).
- 620
- 621 38. VB Bulchandani, R Vasseur, C Karrasch, JE Moore, Solvable hydrodynamics of quantum integrable systems. *Phys. Rev. Lett.* **119**, 195301 (2017).
- 622
- 623 39. L Piroli, J De Nardis, M Collura, B Bertini, M Fagotti, Transport in out-of-equilibrium  $XXZ$  chains: Nonballistic behavior and correlation functions. *Phys. Rev. B* **96**, 115124 (2017).
- 624
- 625 40. V Alba, P Calabrese, Entanglement and thermodynamics after a quantum quench in integrable systems. *Proc. Natl. Acad. Sci.* **114**, 7947–7951 (2017).
- 626
- 627 41. B Doyon, T Yoshimura, JS Caux, Soliton gases and generalized hydrodynamics. *Phys. Rev. Lett.* **120**, 045301 (2018).
- 628
- 629 42. B Doyon, J Dubail, R Konik, T Yoshimura, Large-Scale Description of Interacting One-Dimensional Bose Gases: Generalized Hydrodynamics Supersedes Conventional Hydrodynamics. *Phys. Rev. Lett.* **119**, 195301 (2017).
- 630
- 631 43. X Cao, VB Bulchandani, JE Moore, Incomplete thermalization from trap-induced integrability breaking: Lessons from classical hard rods. *Phys. Rev. Lett.* **120**, 164101 (2018).
- 632
- 633 44. A Bastianello, V Alba, JS Caux, Generalized hydrodynamics with space-time inhomogeneous interactions. *Phys. Rev. Lett.* **123**, 130602 (2019).
- 634
- 635 45. J De Nardis, D Bernard, B Doyon, Hydrodynamic diffusion in integrable systems. *Phys. Rev. Lett.* **121** (2018).
- 636
- 637 46. S Gopalakrishnan, DA Huse, V Khemani, R Vasseur, Hydrodynamics of operator spreading and quasiparticle diffusion in interacting integrable systems. *Phys. Rev. B* **98** (2018).
- 638
- 639 47. A Bastianello, A De Luca, B Doyon, J De Nardis, Thermalization of a trapped one-dimensional Bose gas via diffusion. *Phys. Rev. Lett.* **125**, 240604 (2020).
- 640
- 641 48. JS Caux, B Doyon, J Dubail, R Konik, T Yoshimura, Hydrodynamics of the interacting Bose gas in the Quantum Newton Cradle setup. *SciPost Phys.* **6**, 70 (2019).
- 642
- 643 49. F Moller, et al., Extension of the Generalized Hydrodynamics to Dimensional Crossover Regime. *arXiv e-prints*, arXiv:2006.08577 (2020).
- 644
- 645 50. R Koch, A Bastianello, JS Caux, Adiabatic formation of bound states in the 1d Bose gas. *arXiv e-prints*, arXiv:2010.13738 (2020).
- 646
- 647 51. B Pozsgay, Algebraic Construction of Current Operators in Integrable Spin Chains. *Phys. Rev. Lett.* **125** (2020).
- 648
- 649 52. M Borsi, B Pozsgay, L Pristiyák, Current Operators in Bethe Ansatz and Generalized Hydrodynamics: An Exact Quantum-Classical Correspondence. *Phys. Rev. X* **10** (2020).
- 650
- 651 53. AJ Friedman, S Gopalakrishnan, R Vasseur, Diffusive hydrodynamics from integrability breaking. *Phys. Rev. B* **101**, 180302 (2020).
- 652
- 653 54. J Durnin, MJ Bhaseen, B Doyon, Non-Equilibrium Dynamics and Weakly Broken Integrability. *arXiv e-prints*, arXiv:2004.11030 (2020).
- 654
- 655 55. M Fava, B Ware, S Gopalakrishnan, R Vasseur, SA Parameswaran, Spin crossovers and superdiffusion in the one-dimensional Hubbard model. *Phys. Rev. B* **102** (2020).
- 656
- 657 56. M Schemmer, I Bouchoule, B Doyon, J Dubail, Generalized hydrodynamics on an atom chip. *Phys. Rev. Lett.* **122**, 090601 (2019).
- 658
- 659 57. N Malvania, et al., Generalized hydrodynamics in strongly interacting 1d Bose gases (2020).
- 660
- 661 58. E Ilievski, J De Nardis, Ballistic transport in the one-dimensional hubbard model: The hydrodynamic approach. *Phys. Rev. B* **96**, 081118 (2017).
- 662
- 663 59. H Watanabe, M Oshikawa, Generalized  $f$ -sum rules and kohn formulas on nonlinear conductivities. *Phys. Rev. B* **102**, 165137 (2020).
- 664
- 665 60. H Watanabe, Y Liu, M Oshikawa, On the general properties of non-linear optical conductivities. *J. Stat. Phys.* **181**, 2050–2070 (2020).
- 666
- 667 61. M Ljubotina, M Žnidarič, T Prosen, Spin diffusion from an inhomogeneous quench in an integrable system. *Nat. Commun.* **8**, 16117 (2017).
- 668
- 669 62. E Ilievski, J De Nardis, M Medenjak, T Prosen, Superdiffusion in one-dimensional quantum lattice models. *Phys. Rev. Lett.* **121** (2018).
- 670
- 671 63. S Gopalakrishnan, R Vasseur, Kinetic Theory of Spin Diffusion and Superdiffusion in  $XXZ$  Spin Chains. *Phys. Rev. Lett.* **122** (2019).
- 672
- 673 64. J De Nardis, M Medenjak, C Karrasch, E Ilievski, Anomalous Spin Diffusion in One-Dimensional Antiferromagnets. *Phys. Rev. Lett.* **123** (2019).
- 674
- 675 65. M Ljubotina, M Žnidarič, T Prosen, Kardar-Parisi-Zhang Physics in the Quantum Heisenberg Magnet. *Phys. Rev. Lett.* **122** (2019).
- 676
- 677 66. VB Bulchandani, Kardar-Parisi-Zhang universality from soft gauge modes. *Phys. Rev. B* **101** (2020).
- 678
- 679 67. J De Nardis, S Gopalakrishnan, E Ilievski, R Vasseur, Superdiffusion from Emergent Classical Solitons in Quantum Spin Chains. *Phys. Rev. Lett.* **125** (2020).
- 680
- 681 68. M Rigol, V Dunjko, V Yurovsky, M Olshanii, Relaxation in a Completely Integrable Many-Body Quantum System: An Ab Initio Study of the Dynamics of the Highly Excited States of 1D Lattice Hard-Core Bosons. *Phys. Rev. Lett.* **98** (2007).
- 682
- 683 69. Luca D'Alessio and Yariv Kafri and Anatolii Polkovnikov and Marcos Rigol, From quantum chaos and eigenstate thermalization to statistical mechanics and thermodynamics. *Adv. Phys.* **65**, 239–362 (2016).
- 684
- 685 70. J De Nardis, D Bernard, B Doyon, Diffusion in generalized hydrodynamics and quasiparticle scattering. *SciPost Phys.* **6** (2019).
- 686
- 687 71. B Doyon, Exact large-scale correlations in integrable systems out of equilibrium. *SciPost Phys.* **5**, 54 (2018).
- 688
- 689 72. (year?) See Supplemental Material associated with this manuscript.
- 690
- 691 73. B Doyon, Exact large-scale correlations in integrable systems out of equilibrium. *SciPost Phys.* **5** (2018).
- 692
- 693 74. M Takahashi, *Thermodynamics of One-Dimensional Solvable Models*. (Cambridge University Press), (1999).
- 694
- 695 75. GXW Jiang Yu-Zhu, Chen Yang-Yang, Understanding many-body physics in one dimension from the Lieb-Liniger model. *Chin. Phys. B* **24**, 50311 (2015).
- 696
- 697 76. B Bertini, et al., Finite-temperature transport in one-dimensional quantum lattice models. *Rev. Mod. Phys.* **93**, 025003 (2021).
- 698
- 699 77. T Prosen, Open  $xxxz$  spin chain: Nonequilibrium steady state and a strict bound on ballistic transport. *Phys. Rev. Lett.* **106**, 217206 (2011).
- 700
- 701 78. C Karrasch, JH Bardarson, JE Moore, Finite-temperature dynamical density matrix renormalization group and the drude weight of spin-1/2 chains. *Phys. Rev. Lett.* **108**, 227206 (2012).
- 702
- 703 79. A Bastianello, A De Luca, Integrability-protected adiabatic reversibility in quantum spin chains. *Phys. Rev. Lett.* **122**, 240606 (2019).
- 704
- 705 80. Y Tanikawa, K Takasan, H Katsura, Exact results for nonlinear Drude weights in the spin-1/2  $XXZ$  chain. *arXiv e-prints*, arXiv:2103.05838 (2021).
- 706